The Centre for Australian Weather and Climate Research
A partnership between CSIRO and the Bureau of Meteorology

Assessing Upgrades to the Bureau of Meteorology's Wave Forecasting System using Satellite Altimeter Data

Tom H. Durrant, Diana J. M. Greenslade and Graham R. Warren

CAWCR Technical Report No. 012

June 2009

www.cawcr.gov.au

Assessing Upgrades to the Bureau of Meteorology's Wave Forecasting System using Satellite Altimeter Data

Tom H. Durrant[1], Diana J. M. Greenslade[1] and Graham R. Warren[2]

CAWCR Technical Report No. 012

June 2009

[1] Centre for Australian Weather and Climate Research, a Partnership between the Bureau of Meteorology and CSIRO, Melbourne, Australia
[2] Bureau of Meteorology, Melbourne, Australia

ISSN: 1836-019X

National Library of Australia Cataloguing-in-Publication entry

Author: Durrant, Tom. H., 1981-

Title: Assessing upgrades to the Bureau of Meteorology's wave forecasting system using satellite altimeter data [electronic resource] / Tom H. Durrant, Diana J.M. Greenslade, Graham R. Warren.

ISBN: 9781921605222 (pdf)
Series: CAWCR technical report ; no. 12.
Notes: Bibliography.
Subjects: Ocean waves--Australia--Mathematical models. Ocean waves--Australia--Remote sensing. Marine meteorology--Australia--Mathematical models. Altimeter--Australia--Data processing.
Other Authors/Contributors: Greenslade, Diana J. M., Warren, Graham R. (Graham Ross). Centre for Australian Weather and Climate Research. Australia. Bureau of Meteorology. CSIRO.
Dewey Number: 551.463015118

Enquiries should be addressed to:
Tom Durrant
Centre for Australian Weather and Climate Research:
A partnership between the Bureau of Meteorology and CSIRO
GPO Box 1289, Melbourne
Victoria 3001, Australia

t.durrant@bom.gov.au

Copyright and Disclaimer

Contents

List of Figures

List of Tables

1. INTRODUCTION

The Bureau of Meteorology (the Bureau) currently runs AUSWAM operationally, a version of the third-generation wave model WAM (WAMDI Group 1988). Forecasts of sea-state from AUSWAM are used as numerical forecast guidance for the Bureau's marine services. Details of the current implementation of AUSWAM can be found in (National Meteorological and Oceanographic Centre (NMOC), 2002) and the references listed therein. Of particular relevance here is the directional resolution of the wave spectrum (currently set at 30^o) and the data assimilation (DA) scheme, which includes Significant Wave Height (H_s) data from the Jason-1 satellite altimeter only.

A directional resolution of 30^o is relatively coarse, compared to other global operational wave forecasting systems which are typically twice this at 15^o. Coarse resolutions can save on computational resources but there are potentially major negative impacts on the resulting wave forecasts. In particular, a coarse directional resolution constrains the wave energy to propagate in a limited number of directions. This can lead to undesirable features as, for example, swell propagates long distances across the ocean surface and results in "clumping" of the wave energy, known as the "sprinkler effect". There are various techniques that can be used to minimize the sprinkler effect – e.g. increasing the angular resolution of the wave spectrum by including more directional bins, adding diffusion to the propagation terms, etc. (Tolman, 2002). Future plans within the Bureau's operational systems involve potentially replacing the current wave model, so for the time being, we consider the simplest method, which is to increase the angular resolution.

In addition to the Jason-1 observations, the Bureau currently receives H_s data in real-time from the Envisat satellite altimeter, so the opportunity exists to expand the DA system by including this source of data. One of the main limitations of assimilating satellite altimeter data is the sparseness of the data, so including observations from two satellites with different orbit characteristics, and thus different sampling patterns, could be expected to improve the skill of the wave forecasts.

Traditionally, in situ buoy data are used to verify the impact of potential upgrades to the wave modelling system, such as those described above. The root-mean-square (RMS) difference between model forecast and buoy H_s is typically used as a "skill score". If the RMS can be reduced, this is seen as a positive gain for the wave model system and the change is duly implemented (e.g. Greenslade and Young, 2005). The advantage of using buoy observations to verify the model forecasts is that they are not used in the DA system and represent an independent data source.

However, the use of buoy data alone for model verification does have its limitations. Buoy data typically are only available near the coast, so while modelled H_s may be improved at those particular areas, it may not be true everywhere in the domain. It could be argued that wave model skill in the high seas regions is just as relevant for the Bureau's Marine Services as skill at the coast, so this is a particular deficiency of using in situ buoy data alone to verify model changes.

To address these issues, a new technique for verifying the wave model is developed using satellite altimeter data over the open ocean. The global coverage makes these observations ideal for model evaluation and the diagnosis of potential model errors. The Fast-Delivery (FD) altimeter products used here are received at the Bureau within three hours of observation. In previous work (Durrant et al.,2009), FD H_s from both the Jason-1 and Envisat altimeters has been validated against in situ buoy data and appropriate correction schemes have been derived. In this work, these results are applied to the altimeter data streams and these are then used to assess the two potential upgrades to the wave forecasting system discussed above.

2. METHOD

The changes to AUSWAM that are evaluated here are a) a doubling of the directional resolution of the wave model spectrum and b) the incorporation of Envisat H_s data in addition toJason-1 in the DA system. These potential upgrades require increases in computational requirements, so any resulting improvements in forecast skill are considered in this context.

Several model runs were performed over the month of January 2005. All model runs were on the global domain (0-360^o, 78^{o}S – 78^{o}N) at 1^o spatial resolution. All runs used the same wind forcing fields from the Bureau's global atmospheric model and the same initial conditions (a one month spin up was performed for each of the two options for directional resolution).72-hour forecasts were made every 12 hours, after a 12-hour hindcast period, during which DA was performed (for the DA runs). DA was performed as in the current operational system (Greenslade and Young, 2005). Throughout this section, the altimeter data are corrected according to Durrant at al (2009). Specifically, no correction was applied to Jason-1 and the following small linear correction was applied to Envisat data:

$$H_s^{adj} = 1.085 H_s^{FD} - 0.213m \quad (1)$$

The model runs were as follows:

Noassim-12:	12 directional bins	No assimilation
Noassim-24:	24 directional bins	No assimilation
Jason-12:	12 directional bins	Assimilation with Jason-1 data only
Jason-24:	24 directional bins	Assimilation with Jason-1 data only
Both-12:	12 directional bins	Jason-1 and Envisat data assimilated
Both-24:	24 directional bins	Jason-1 and Envisat data assimilated

The Bureau operational configuration up until 22nd July 2008, was Jason-12.

Figure 1 shows the data coverage from the two satellites in a typical 3-hour DA period and Figure 2 shows a comparison of the resulting increment fields for the case of assimilating Jason-1 alone, and assimilating both satellites. The increment field shown here is the analysis increment, i.e. the value of H_s at each model grid point that is added to (or subtracted from) the background field in order to produce the analysed H_s field. It can be seen that a considerably larger portion of the global wave field is updated when both satellites are assimilated, so this would be expected to have some impact on the forecasts.

It is also interesting to examine how these increments vary with time. We know that the modelled winds are typically underestimated (Schulz *et al.*, 2007) and that the H_s is also underestimated because of this (Greenslade *et al.*, 2005), so we would expect the initial modelled wave fields, on January 1st after the one month spin-up period, to have a significant negative bias. The DA scheme, starting on January 1st would act to eliminate some of this bias, and since the changes to the wave field brought about by the DA take some days to decay (Greenslade and Young, 2005), then over the month, the magnitude of the increments should decrease. Figure 3 shows a time series of the mean absolute value of the increment for the Both-12 and Both-24 model runs. (This mean value does not include grid-points where the increment is equal to zero, in order to eliminate the impact of variations in the amount of

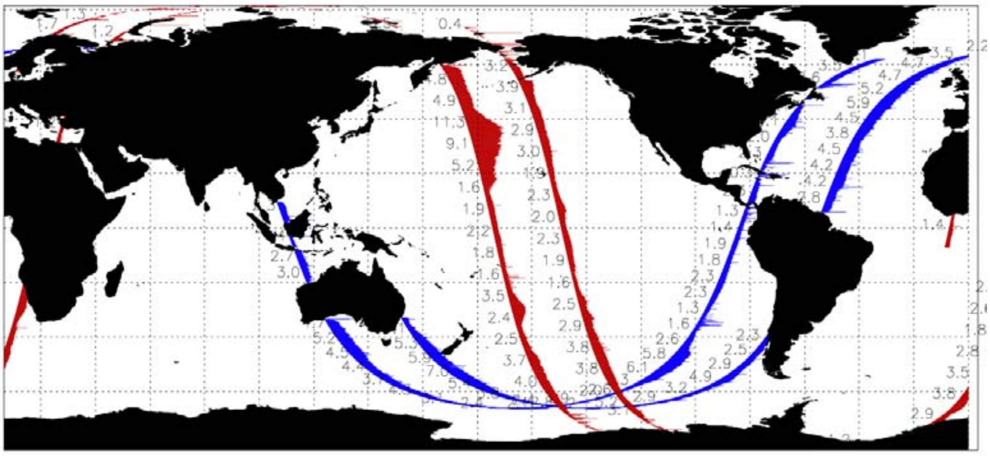

Figure 1 *H_s observations (m) from Jason-1 (blue) and Envisat (red) in a 3-hour time period centred on January 15, 0900Z. The length of the horizontal line indicates observed H_S.*

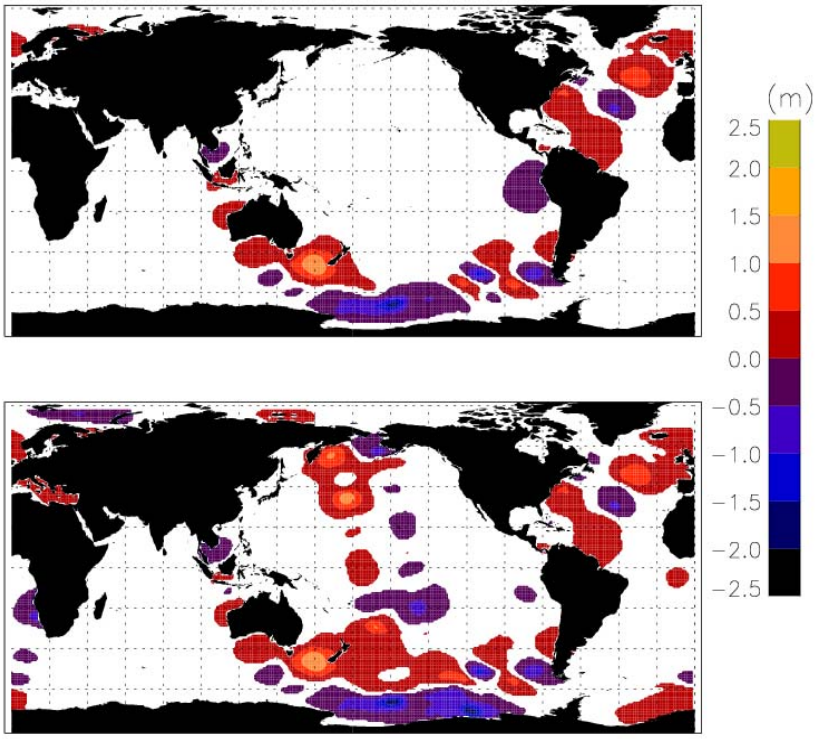

Figure 2 *Increment fields of H_s for the case of Jason-1 data alone (top panel) and both Jason-1 and Envisat (bottom panel) for the data shown in Figure 1, i.e., the assimilation period January 15, 0900Z.*

altimeter data for each assimilation period). We see that this is indeed the case: the magnitude of the increment is relatively large for the first few assimilation periods, then over the first week the increments become smaller and for the remainder of the month they oscillate around a value of approximately 0.13m.

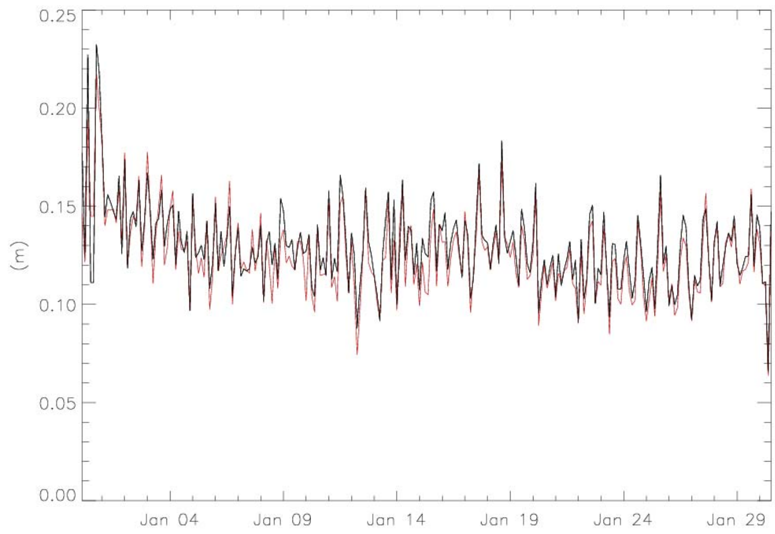

Figure 3 *Time series of the mean absolute value of the increment field for Both-12 (black) and Both-24 (red) model runs.*

Figure 3 also shows a comparison of the increments between the runs with different directional resolution, but the same amount of altimeter data. One expected result of increasing the directional resolution is that the model should distribute the wave energy more accurately over the model grid, and so the corrections needed from the DA should be lower. Indeed, the mean value of the increments over the time period for Both-12 is 0.130 m while the mean value for Both-24 is 0.125 m; a reduction of about 4%.

The skill of each model run is evaluated here by comparison with observations – firstly with *in situ* buoy data in the Australian region and secondly, evaluations against global altimeter observations are performed.

3. EVALUATIONS AGAINST BUOY DATA

The locations of the buoys used for verification of the model runs in this work are shown in Figure 4. Only buoys in the Australian region located in water deeper than 40 m are used here. Observations of H_s are available from some of the buoys at half-hourly intervals (55040, 55026 and 55035), some of the buoys at hourly intervals (55018, 55019, 55022, 55014, 55020) and the remainder at 3-hourly intervals. Linear interpolation in time was used to compare the time series of H_s from each buoy to the 3-hourly time series of H_s at the closest model grid point from each run. Figure 5 shows, for example, the time series of 24-hour forecasts at buoy 55026. The underestimation of H_s from the model runs without DA can clearly be seen here and the DA significantly improves the overall model bias at this location. Note that the increase in the directional resolution of the wave spectrum has also reduced the bias slightly.

Figure 4 *Locations of the buoys used for verification of the model runs*

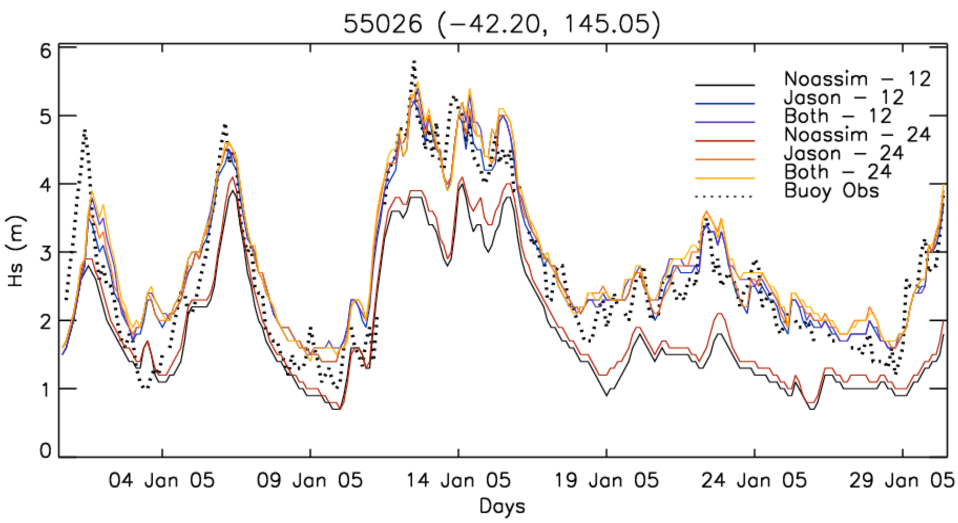

Figure 5 *Time series of H_s at buoy 55026 and the modelled 24-hour forecasts.*

The verification statistics used here are the bias, RMS difference, Scatter Index (SI) and correlation coefficient (R), defined as follows:

$$Bias = \frac{1}{N}\sum_{i=1}^{N} M_i - O_i \tag{2}$$

$$RMS = \sqrt{\frac{1}{N}\sum_{i=1}^{N}\left(M_i - O_i\right)^2} \tag{3}$$

$$SI = \frac{\sqrt{\frac{1}{N}\sum_{i=1}^{N}\left(\left(M_i - \overline{M}\right) - \left(O_i - \overline{O}\right)\right)^2}}{\overline{O}} \tag{4}$$

$$R = \frac{\sum_{i=1}^{N}\left(M_i - \overline{M}\right)\left(O_i - \overline{O}\right)}{\sqrt{\sum_{i=1}^{N}\left(M_i - \overline{M}\right)^2\left(O_i - \overline{O}\right)^2}} \tag{5}$$

Where O_i is the observed H_s, M_i is modelled H_s, N is the number of co-locations and an overbar represents the mean value.

These statistics are calculated for all model runs and 4 different forecast periods: hindcast, 24-hour, 48-hour and 72-hour forecasts. Note that the model output is archived every 12 hours at 3-hourly intervals, so the 24-hour forecast, for example, will actually consist of a recurring series of 15-, 18-, 21- and 24-hour forecasts. Statistics are calculated on the set of all buoys, resulting in 2424 co-locations for each forecast period. Figure 6, for example, shows the co-located buoy and model H_s for all buoys for the 24-hour forecast from the Jason-12 model run. The verification statistics are also shown in this figure and demonstrate that overall, these forecasts have a small (15 cm) positive bias relative to the buoys and an RMS difference of 51 cm. Statistics for all model runs are shown in Figure 7.

There are several points of interest in these summary statistics. Firstly, it can be seen that overall, the bias for the DA cases is positive – particularly for the hindcast and short forecast ranges. Upon inspection of the statistics for individual buoys, it was found that these high positive bias values are dominated by buoys 56004 and 56005 on the West Australian coastline. These are in the shallowest water (between 40 and 50m) so the overestimation of H_s at these locations could be due to shallow water effects, i.e., the observed H_s may be reduced at these locations due to bottom friction, but the model doesn't capture this as it does not incorporate shallow water physics. It should be noted, however, that this positive bias does occur (but to a much lesser extent) at almost all buoy locations, so shallow water effects are unlikely to be the only contributor. An alternative explanation could be that the positive bias is an artefact of simply choosing the closest model grid point in a relatively coarse (1^{o}) grid, as opposed to interpolating the model fields. This would result in a positive bias because the model grid point is always further offshore than the coastal buoy location, and H_s typically increases with distance from the coast. Alternatively, it could be an actual effect – the DA is perhaps over-compensating somehow for the negative bias in the non-assimilated fields. This will be discussed further in the next section, where the model runs are compared to the altimeter data.

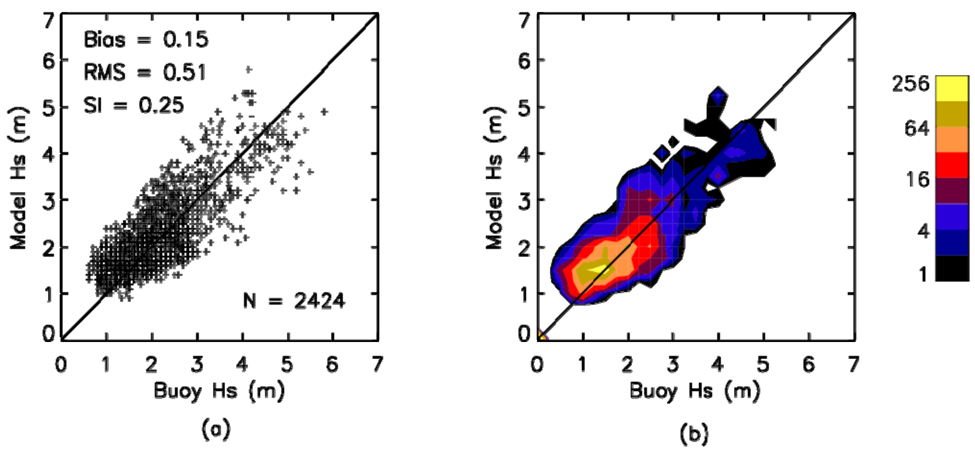

Figure 6 *Co-located buoy and model H_s for the Jason-12, 24 hour forecast for all 12 buoys. (a) shows co-locations, (b) shows the number of co-locations in each 0.5 m bin contoured.*

Increasing the directional resolution increases the overall H_s (discussed further in Section 4). In the case of the no assimilation runs, this reduces the negative bias, although for the DA runs, it increases the positive bias. It has also reduced the variable errors in the run with no DA, as seen in the SI, so this suggests that it is an improvement overall. However, it appears from the SI results that if the directional resolution of the current model implementation is increased (i.e. Jason-12 to Jason-24), then the variable errors are only improved for the longer forecast ranges.

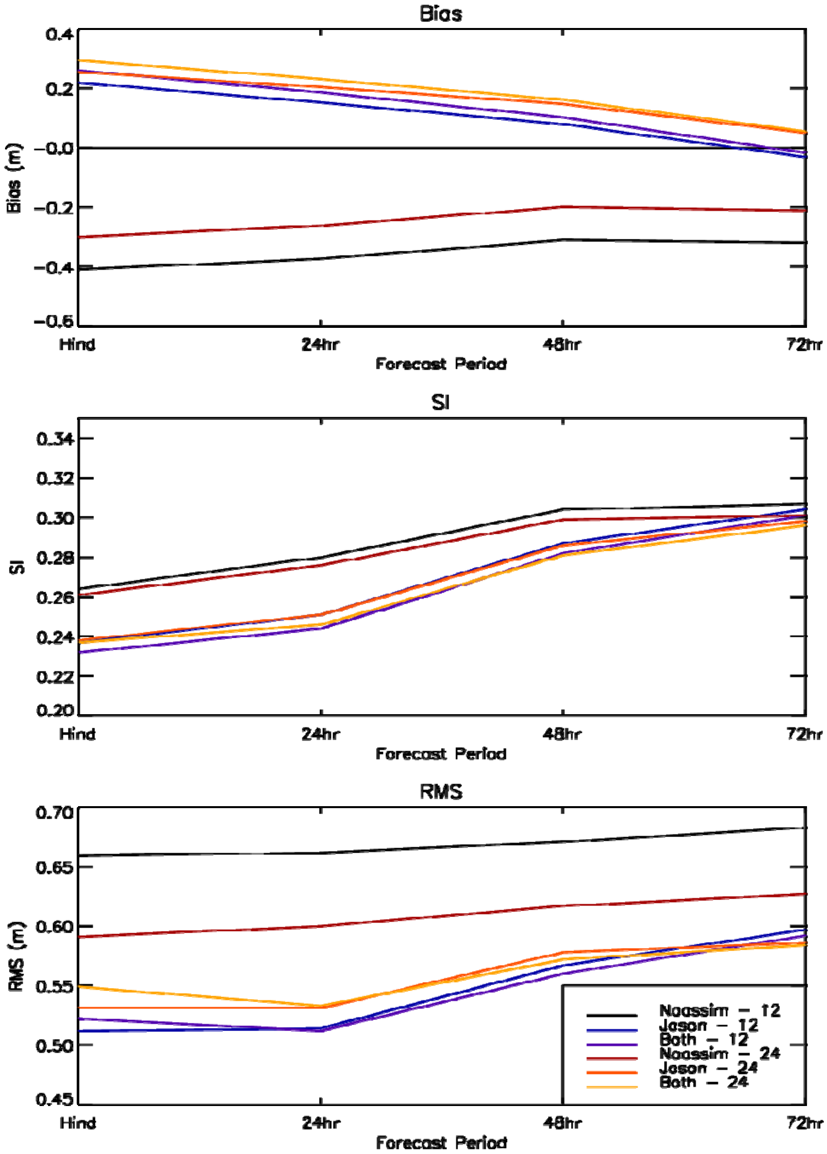

Figure 7 *Summary of verification statistics (Bias, Scatter Index and RMS difference) for all model runs compared to the buoys shown in Figure 4.*

This is also true for the case of assimilating both satellite data streams – in fact, in this case, the lowest variable errors are from the model run with the coarser directional resolution. A possible explanation for this is that the directional increase has only a small impact, but it is effective for all forecast periods. For the short range forecasts, the DA improvement dominates the verification statistics, so it is only for the longer range forecasts, when the impact of the DA has decayed that gains are made by increasing the directional resolution.

Examining the RMS alone suggests that the increase in directional resolution is detrimental. However, this is largely due to the increase in the positive bias that this change brings, which, as discussed above, may or may not be a true assessment of the model's performance.

3.1 Operational Trials

In addition to the verifications against buoy data performed here, a parallel trial testing these implementations was performed in NMOC. This was done during the first half of 2008 and mirrors the operational system. This system consists of a global model, a higher resolution nested regional model and a further higher resolution nested mesoscale model covering the Australian coastline. Further details of the operational system can be found in (NMOC, 2002). Only the global model and the full Australian regional model include DA. Trial forecasts were performed in real-time and the data cut-off time for observations used in the DA system was the same as that for the operational models.

Initially the trial system was run with the same spectral resolution as the operational system but including the (corrected) Envisat data in the DA step as well as the Jason-1 data. The systems were run for a period of about 6 weeks in January/February 2008. The results were inconclusive with very little change in the performance compared with the buoy measurements. However, as there was no degradation in performance it was decided that it would be beneficial to include the Envisat data as well. Since the DA step does improve the wave model forecast, the inclusion of the second altimeter data stream will provide some redundancy in the observations used, protecting against failure of either of the instruments or the communications which deliver the data.

The more intensive trial involving the increase in the angular resolution of the wave spectrum commenced in March 2008. Results are presented here for the period 17 April – 16 July 2008. Shown in Figure 8 is the comparison between the verification results for the existing operational model and the upgraded configuration. As was the case in the January 2005 results discussed above, a slight increase in the bias across all forecast periods is evident, resulting in an increased positive bias for short range forecasts, and a decreased negative bias for long range forecasts. Despite this, RMS is improved for all periods, suggesting that the variance of the wave field is better captured in the upgraded system. For the regional and mesoscale systems, while there is little change in the RMS error, the existing positive bias for all forecast periods has been increased. While RMS does not decrease, as with the global model, it remains almost unchanged, again suggesting improvements in the variance.

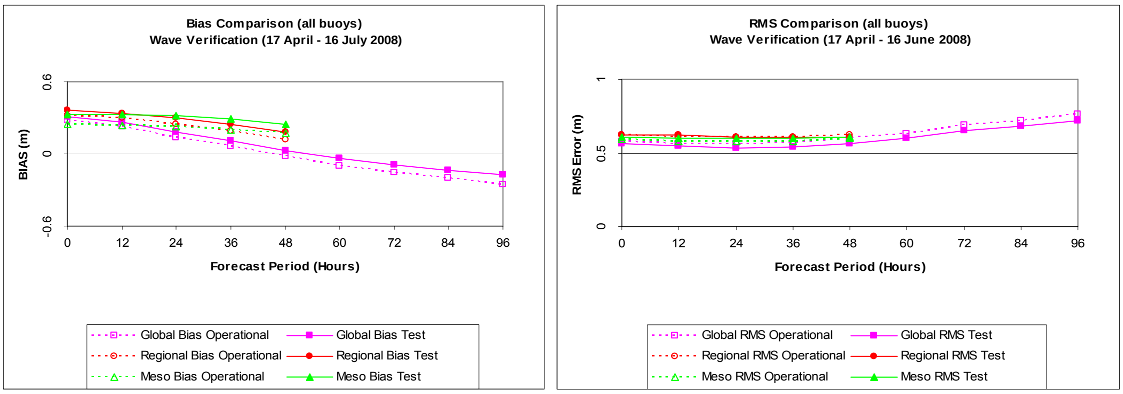

Figure 8 *Bias (left) and RMS error (right) of the wave model forecasts compared to wave observations around the Australian coast.*

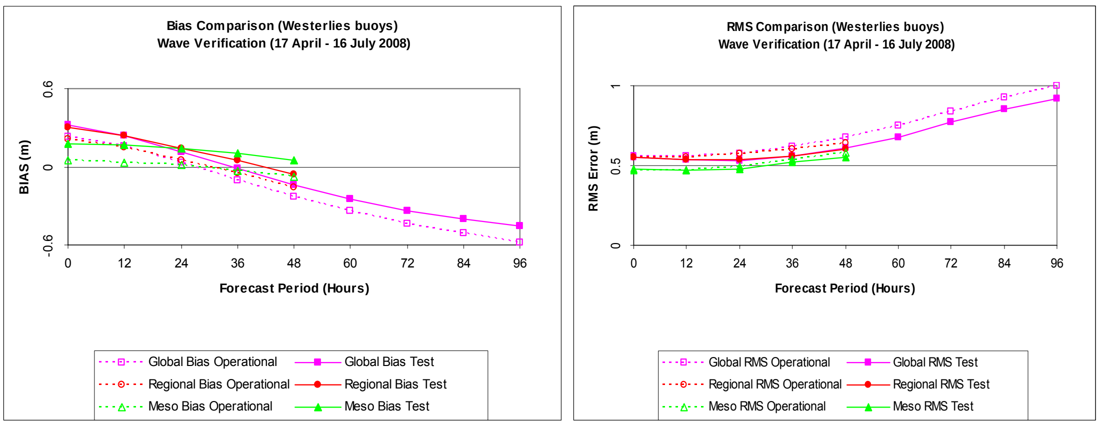

Figure 9 *As for Figure 8 but for wave observations exposed to westerlies.*

Both the increase in bias and the decrease in variance are likely due to the increase in angular resolution resulting in better propagation of the swell components. At this time of year, swell generally originates in the high latitude westerlies to the south of the Australian continent, hence, buoys located on the west and south coasts might be expected to show a stronger signal than those on the east coast. Figure 9 shows results for west and south coast buoys only (55026, 55040, 56004, 56005, 56006, 56008). Relative to the results for all buoys, these indeed show both larger increases in bias, and larger decreases in RMS.

There are slight differences between the results seen in the January 2005 analysis, and that of the operational trials. For example, the positive bias seen in the January 2005 results is greater than that seen in the operational trials. This could in part be explained by the fact that the operational verification system uses a cubic spline fitting to interpolate (or extrapolate in the case of adjacent land point) the model output to the buoy location. These validations also occur over different time periods, with the first analysis performed for January 2005 and the operational trial in April to July of 2008. In addition to the seasonal differences, the atmospheric model has undergone several upgrades in this time (NMOC, 2008) and thus the error characteristics of the wave model from these different periods might be expected to differ. In both cases, a positive bias exists for the wave model relative to the observational data from the buoys.

4. EVALUATION AGAINST ALTIMETER DATA

Even though the altimeter data are directly used in the DA, they can still be used as an independent data source for verification of the forecasts due to their diminishing influence throughout the forecast period. In this section, the two altimeter data streams are combined and treated as one data source. This provides good spatial coverage over the oceans during the one month period of January 2005. Statistics are calculated within 10^o by 10^o boxes at 5^o intervals over the globe. Raw data produced by satellites often contain errors, and must be adequately quality controlled before use. During DA, the method of Young and Glowacki (1996) is used, consisting of an initial check for gross error against the first guess field, followed by a cross validation check for consistency with other nearby data. This serves to remove erroneous data, with the comparison with the first guess field also limiting shocks to the model. For the validation data stream, quality control is done independently of the model. A check is performed based on the standard deviation of the 20Hz and 10Hz H_s values for Jason-1 and Envisat respectively (Mackay, 2008), and nearest neighbour comparisons are performed to remove any remaining obvious errors. In order to match the spatial scales of variability between model and observations, "super-obs" are then calculated by performing 1^o along track averages, consisting of 15-20 individual observations. Figure 10 shows several Jason-1 tracks of (a) raw, (b) quality controlled and (c) super-obbed data.

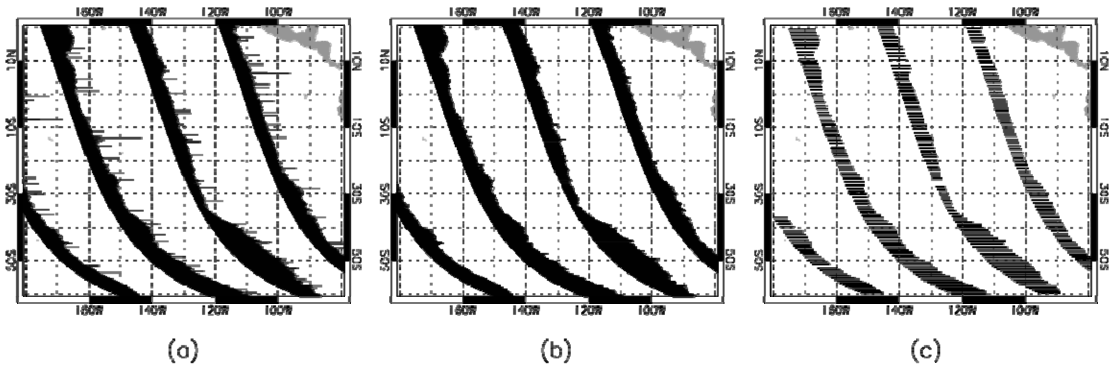

Figure 10 *Jason-1 passes showing (a) raw data, (b) quality controlled data and (c) super-obbed data. The length of the horizontal line indicates observed H_S.*

Model data is bi-linearly interpolated in space to the altimeter observation location, and linearly interpolated in time to make up a set of co-locations. For each 10^o by 10^o box, co-locations are then accumulated for the month period, and statistics calculated from these co-locations. Figure 11 shows the mean bias over the month for the 24-hour forecasts from the Noassim-12 run. The model is biased low over almost the entire domain, reaching more than 1 m in some areas. In general, the largest negative biases exist in mid-to-high latitudes, where the H_s is highest.

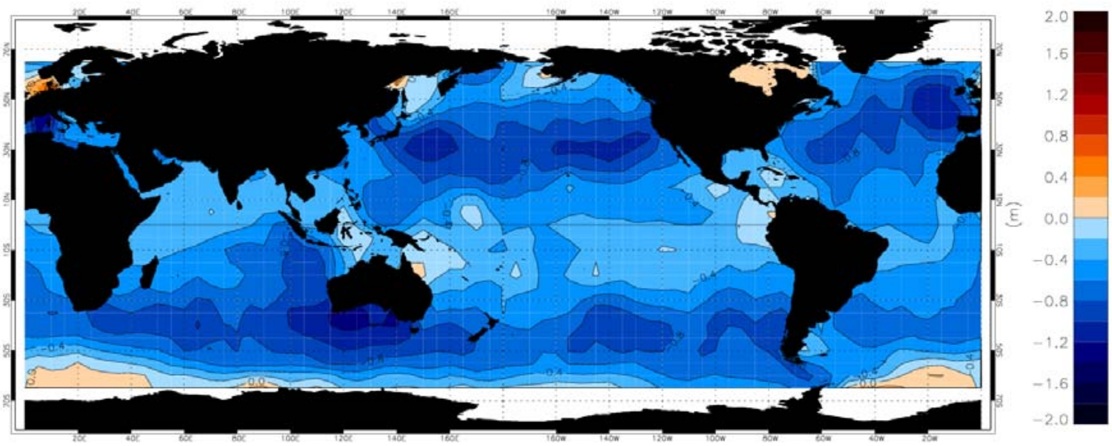

Figure 11 *Bias (modelled H_s - altimeter H_s) for 24-hour forecasts from the Noassim-12 model run.*

The DA would be expected to remove a large part of this bias. This can be seen in Figure 11, which shows the bias for the run with twelve directional bins and both satellite data streams assimilated (Both-12). Most of the areas of high negative bias have disappeared and there are some areas, mainly in the tropics, where in fact the model now has a positive bias. As discussed in Section 3, buoy verifications show a positive bias in the model for the DA cases, particularly on the west coast of Australia. These altimeter results do not show this same bias. It is unclear why this is the case, though it is suggested that the wave field at some buoy locations may be experiencing coastal effects such as sheltering or bottom friction, that are unresolved by the model. These altimeter results suggest that the model is performing better than was previously estimated from buoy observations alone.

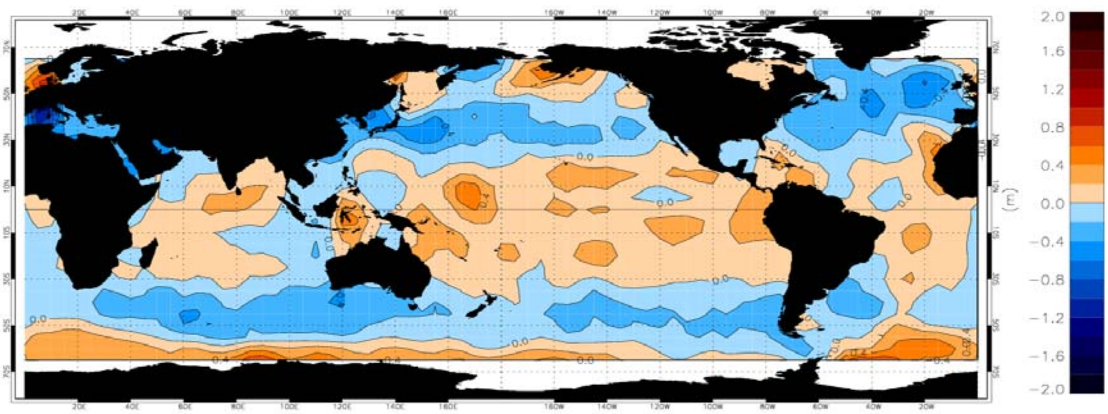

Figure 12 *Same as Figure 11 except for the Both-12 model run.*

Figure 13 (a) shows the spatial distribution of the SI from the Jason-12 model run, as compared to the satellite data. Recall that SI is the square root of the variance of the difference between the observed H_s and the model H_s normalised by the mean observed H_s. It is important to note here that while we have been assuming that the altimeter data are unbiased (this is a reasonable assumption based on the results in Durrant et al, 2009) we can not similarly assume that the altimeter observations have no variable errors. The variance upon which the SI here is based is therefore the sum of the model error variance and the altimeter error variance. The aim of this section is to compare the error characteristics of different model runs and since the altimeter error variance will not change between each run, we can still use these results for comparison purposes.

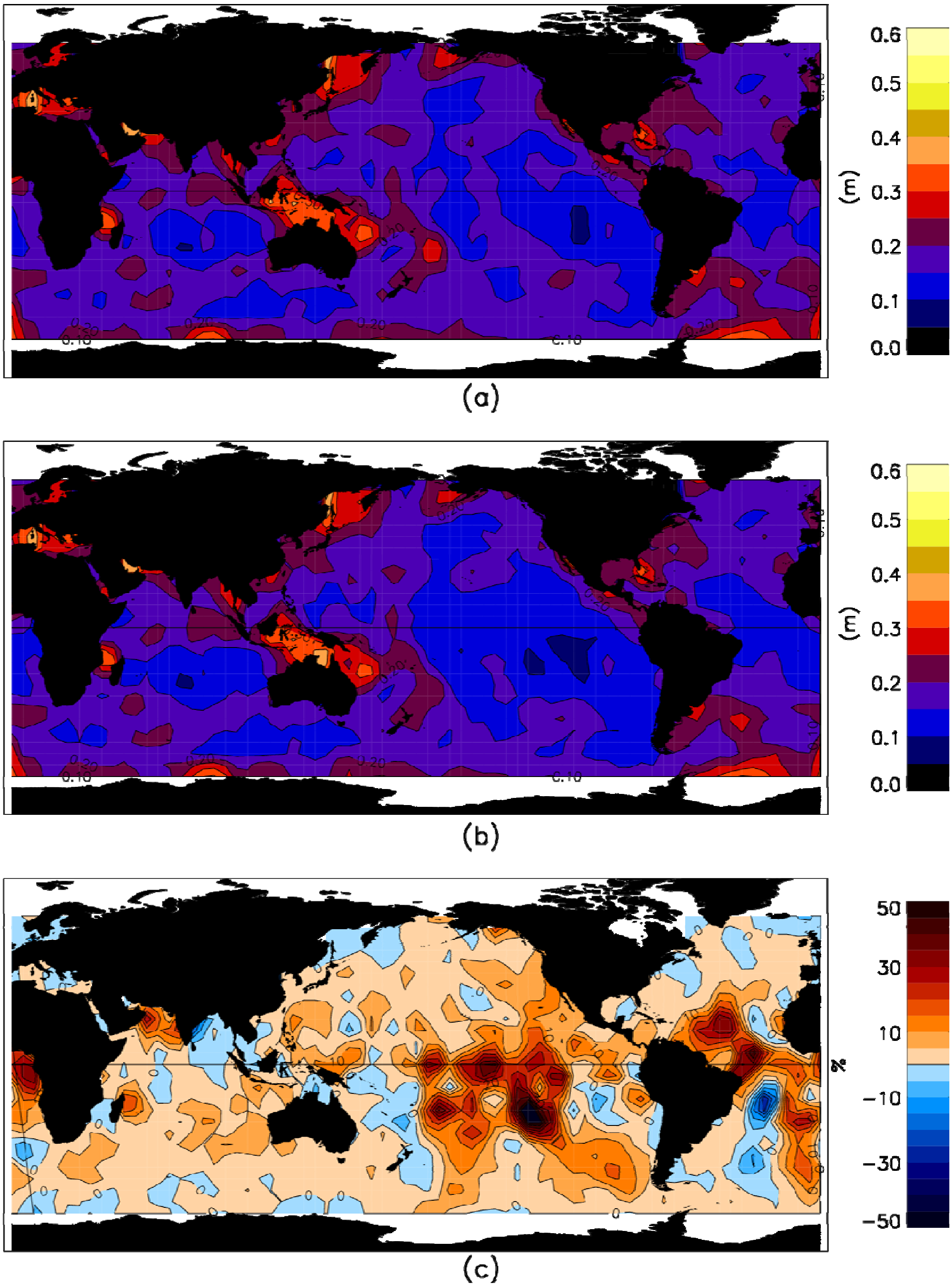

Figure 13 *Scatter Index for 24-hour forecasts from the (a) Jason-12 and (b) Jason 24 runs. (c) shows the percentage improvement from (a) to (b).*

Due to the normalised nature of this statistic, errors are fairly consistent over the major ocean basins. Areas of high SI can be seen around, and in the wake of, islands north of Australia and around South East Asia for example. This is likely due to modelled wave energy propagating incorrectly through islands that are unresolved by the relatively coarse 1^o grid. Figure 13 (b) shows SI for the Jason-24 run, i.e. the same as Figure 13 (a), only with the directional resolution increased from 12 to 24 bins. This shows generally lower SI over most of the globe, reflecting the positive impact of this change. Figure 13 (c) shows the percentage improvement resulting from this increase in directional resolution. This shows the greatest improvements in the central and south eastern Pacific region with up to 50% improvement. This is consistent with better propagation of North Pacific winter storm swells resulting from a reduction in the sprinkler effect.

Overall statistics for all model runs are shown in Figure 14. Rather than calculating these statistics simply from the set of all altimeter/model co-locations over the globe, they are calculated by averaging together the statistics calculated from each 10^o by 10^o box. While it could be argued that this is not the most statistically robust method, this approach was taken here in the interests of gaining the best overall global picture. Figure 15 shows the number of individual model/altimeter super-obbed co-locations in each 10^o box. Simply using the entire set of co-locations to calculate the statistics would give a higher weighting to the high latitudes where the density of observations is greatest due to the convergence of the altimeter tracks. In addition, the statistics for each box (i.e. the bias, RMS etc.) are normalised according to latitude. This avoids placing too much emphasis on the statistics of 10^o boxes at higher latitudes, which are considerably smaller than 10^o boxes at the equator.

Some of the features of these verifications are similar to those of the buoy verifications, while there are also some major differences. In Figure 14 for example, consider first the bias statistics. As for the buoy verifications, increasing the directional resolution increases the bias over all forecast periods. Inspection of the spatial distribution of the bias shows this increase to be consistent over the globe. This is possibly due the fact that increasing the directional resolution of the wave spectrum reduces the sprinkler effect and allows propagation of wave energy to a greater number of model grid points. This will therefore result in an increase in the overall H_s. Another explanation could be that the change in directional resolution changes the amount of shadowing due to islands. Whatever the reason, these results demonstrate that increasing the directional resolution of the wave spectrum has more of an impact than simply improving the aesthetics of the modelled wave fields, as suggested in WISE Group (2007). This discrepancy could be because here we are considering a change in directional resolution from 30^o to 15^o, rather than from 15^o to higher resolution. In addition, the sprinkler effect is more pronounced in AUSWAM due to the higher-order propagation numerics. Clarification of these results deserves further investigation.

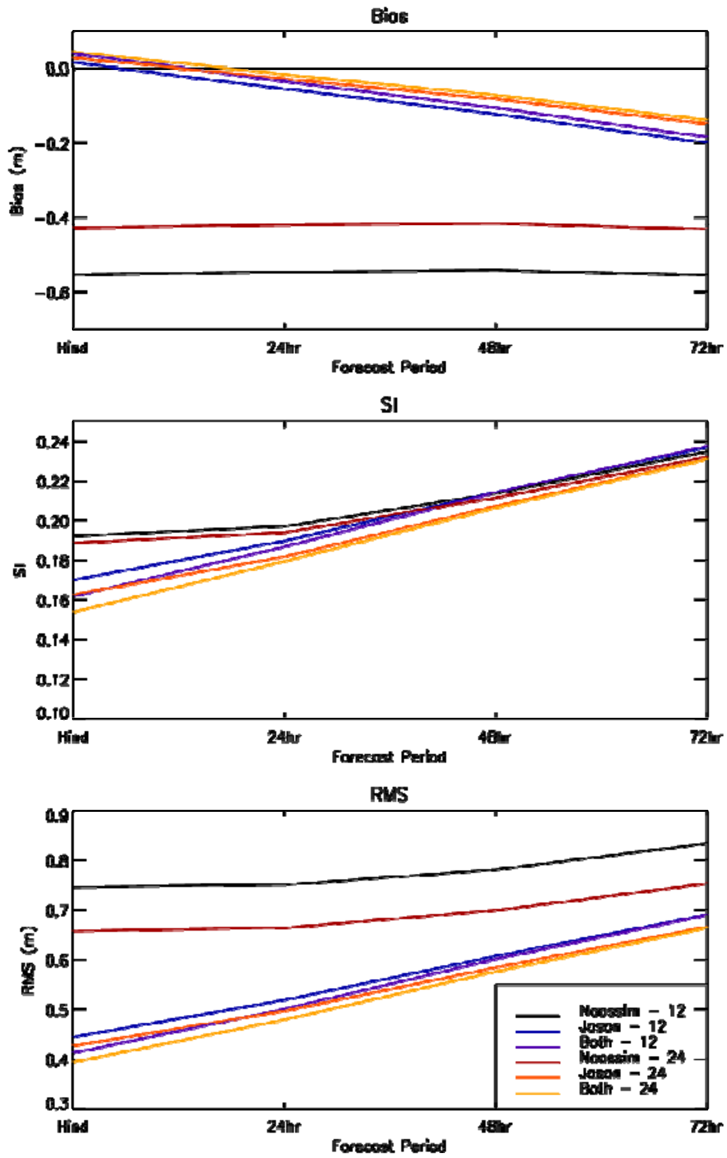

Figure 14 *Summary of verification statistics (Bias, Scatter Index and RMS difference) for all model runs compared to Jason-1 and Envisat satellite altimeter observations.*

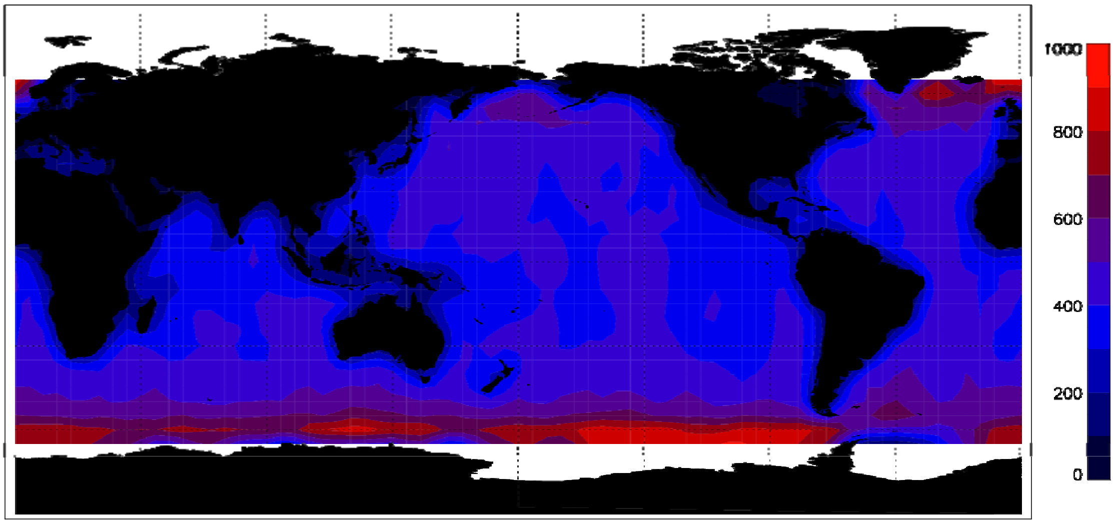

Figure 15 *Number of model/altimeter co-locations in each 10^o by 10^o box.*

Note that all the DA runs have a bias that is very close to zero for the hindcasts. This is mainly a reflection of the fact that the hindcasts are not actually independent of the observations that they are being compared to. However, it is worth emphasizing (see Figure 12, for example) that zero bias overall does not mean that the bias is zero everywhere, and in fact the model bias does vary substantially over the globe. The SI results in Figure 14 clearly show the benefit of both additions to the operational system. The picture here is clearer than that of the buoy comparisons, with the case of both altimeter data streams being assimilated and 24 directional bins producing the lowest SI throughout the forecast period. At the short-range forecasts (less than 24 hours) the results are as expected – DA cases reduce the variable errors in the model fields, and the assimilation of both altimeters yields better results than Jason-1 only. As the forecast period increases, the importance of the increased directional resolution becomes increasingly apparent, with very little impact from the DA evident by the 72 hour forecast. These results present a strong case for incorporating both changes into the operational system.

5. COMPUTATIONAL USAGE

Table 1 shows a summary of the computational usage on the NEC SX6 for each model run. The User time is the average number of CPU seconds for a 12-hour hindcast period and a 72-hour forecast period. Note that all timings are based on running the model on a single processor - these may be different for multi-processor computation.

Table 1 *Computational usage summary for each model run. Jason-12 is highlighted as the current operational configuration.*

Run	User time (sec)	Memory size (MB)
Noassim-12	430	1296
Noassim-24	838	2512
Jason-12	*664*	*1312*
Jason-24	1070	2528
Both-12	1110	1312
Both-24	1324	2528

The assimilation of Jason-1 data increases the time taken by around 50%. In other words, for a 12-hour hindcast and 72-hour forecast the assimilation of Jason-1 data takes up around one third of the total time. When Envisat is included as well, the time increases substantially and the DA is almost two thirds of the total time.

The increase in the spectral resolution from 12 to 24 directional bins doubles the memory size required, not surprisingly. This also doubles the time taken for the run without DA. For the DA runs, the increase in time due to the increase in directional resolution applies only to the non-DA component of the total time, so the impact is not so large. For Jason-1 alone, the increased spectral resolution increases the time by 60% and if data from both satellites is assimilated, the increase in resolution increases the time by only 20%.

6. SUMMARY AND FURTHER WORK

Corrected near-real-time altimeter data have been used to make preliminary assessments of two potential upgrades to the Bureau's wave forecasting system – specifically, an increase in the directional resolution of the wave spectrum and the expansion of the data assimilation system to include Envisat H_s data as well as Jason-1. *In situ* buoy data were also used to assess the improvements in model forecast skill and the computational requirements of the potential upgrades were evaluated.

Various issues associated with the verification techniques were discussed, such as the proximity of the buoys to the Australian coast, and the error variance of the altimeter observations. The conclusions from the buoy verifications were that for short ranges, the best results would be obtained from assimilating both sets of altimeter data, while for longer range forecasts, the best results are obtained from the increased directional resolution. The DA runs showed a positive bias relative to the buoys, especially on the west coast. Verification against the altimeter data does not show this bias, suggesting that it is possibly a coastal effect.

These verifications also showed that, for the non-DA case, the large negative bias in the modelled wave fields is somewhat reduced by the increase in the directional resolution. For the DA cases, this bias was largely eliminated when averaged over the globe, however regional biases remained. Overall, the altimeter verifications suggested that both upgrades produce clear and consistent improvements in model performance, with the Both-24 run achieving the lowest SI and RMS.

These verifications have provided some interesting results that deserve further investigation. For example, there is a ubiquitous decrease in the negative bias that occurs when the directional resolution is increased. It would be interesting to assess to what extent this occurs for different spatial and directional model resolutions.

This study has focused mainly on the global implementation of AUSWAM. The operational trial considered the higher resolution nested models as well, but these models were not considered in the altimeter verifications. There has been an inherent assumption that if the global model skill is improved, this will also feed into better regional model forecasts. This would occur because a) the enhancements made on the global scale are assumed to also be effective at the regional scale and b) an improved global model provides higher quality boundary conditions for the nested models. While the operational trials include some analysis of the regional systems, an altimeter based spatial analysis is certainly warranted.

Knowledge of the spatial variation of both bias and variable error provides a powerful tool for wave model diagnostics although it is only used here to gauge overall improvement in model performance. As wave energy can travel over entire ocean basins, it is difficult to isolate errors associated with local growth, dissipation and propagation when using separate point observations such as buoys. The altimeter based verification scheme developed here has been found to be a robust system for determining such information.

The spatial distribution of the bias seen in these results is likely to be due to either errors in the winds used to force the wave model, or deficiencies in the wave model physics. Satellite scatterometers provide an ideal source of marine wind observations and once the characteristics of the wind forcing errors are known, then the wave model physics can be considered more closely. This is also planned for further work, and will be especially relevant in the context of a new atmospheric model that is planned for operational implementation at the Bureau in the near future. A knowledge of the spatial biases in the wind, in concert with the altimeter verification scheme developed here provides a powerful platform for model diagnostics and development.

ACKNOWLEDGEMENTS

The authors would like to thank Jean-Michel Lefevre (Meteo-France), and the European Space Agency for providing some Jason-1 and Envisat data. We would also like to thank Mark Hemer and Eric Schulz for their comments on the manuscript.

REFERENCES

Durrant, T., Greenslade, D.J.M. and I. Simmonds, 2009: Validation of Jason-1 and Envisat Remotely Sensed Wave Heights, *J. Atmos. Oc. Tech.*, **26, No. 1**, pp 492 - 502

Greenslade, D.J.M. and I.R. Young, 2005: The impact of inhomogenous background errors on a global wave data assimilation system, *J. Atmos. Oc. Sci.*, **10, No. 2** doi:10.1080/17417530500089666.

Greenslade, D.J.M., E. W. Schulz, J. D. Kepert and G.R. Warren, 2005: The Impact of the Assimilation of Scatterometer Winds on Surface Wind and Wave Forecasts, *J. Atmos. Oc. Sci.*, **10, No 3**, doi:10.1080/17417530600784976

Mackay, E. B. L.; Retzler, C. H.; Challenor, P. G. & Gommenginger, C. P. A parametric model for ocean wave period from Ku band altimeter data. *Journal of Geophysical Research*, 2008, **113**, C03029

National Meteorological and Oceanographic Centre, 2002: Changes to the Operational Sea State Forecast System, *Analysis and Prediction Operations Bulletin No. 55*, Bur. of Meteorology.

National Meteorological and Oceanographic Centre, 2008: Operational Upgrade of GASP to 60 levels**,** *Analysis and Prediction Operations Bulletin No. 73*, Bur. of Meteorology.

Schulz, E. W., J. D. Kepert, and D. J. M. Greenslade, 2007: An Assessment of Marine Surface Winds from the Australian Bureau of Meteorology Numerical Weather Prediction Systems, *Wea. and Forecasting*, **22, No. 3**, pp 609 - 632.

Tolman, H L., 2002: Alleviating the Garden Sprinkler Effect in wind wave models, *Ocean Modelling*, **4**. pp 269 – 289.

WAMDI Group (S. Hasselmann, K. Hasselmann, E. Bauer, P.A.E.M. Janssen, G. Komen, L. Bertotti, P. Lionello, A. Guillaume, V.C. Cardone, J.A. Green-wood, M. Reistad, L. Zambresky, and J.A. Ewing), 1988: The WAM model - A third generation ocean wave prediction model. *J. Phys. Oceanogr*., **18**, 1775-1810.

WISE Group (Cavaleri L., J.-H. Alves, F. Ardhuin, A. Babanin, M. Banner, K. Belibassakis, M, Benoit, M. Donelan, J. Groeneweg, T.H.C. Herbers, P. Hwang, P.A.E.M. Janssen, T. Janssen, I.V. Lavrenov, R. Magne, J. Monbaliu, M. Onorato, V. Polnikov, D. Resio, W.E. Rogers, A. Sheremet, J. McKee Smith, H.L. Tolman, G.van Vledder, J. Wolf, I. Young), 2007: Wave modelling – the state of the art, *Progress in Oceanography, in press*.

Young, I. R., and T. J. Glowacki, 1996: Assimilation of altimeter wave height data into a spectral wave model using statistical interpolation, *Ocean Eng*., **23(8)**, 667– 689.

The Centre for Australian Weather and Climate Research is a partnership between CSIRO and the Bureau of Meteorology.